Atomic and electronic structure of single and multiple vacancies in GaN nanowires from first-principles

Damien J. Carter and Catherine Stampfl*

School of Physics, The University of Sydney, Sydney, New South Wales 2006, Australia

(Received 24 November 2008; revised manuscript received 18 March 2009; published 1 May 2009)

We present a comprehensive first-principles investigation of single and multiple gallium and nitrogen vacancies in gallium nitride (GaN) nanowires. We consider nanowires in the [0001] growth direction, with diameters of 9.5 and 15.9 Å and investigate the stability of multiple vacancies for a wide range of configurations to determine the preferred spatial distribution. The influence of saturating the dangling bonds at the edge of the nanowires is also investigated. For one, two, and three nitrogen vacancies, we find that the most favorable configuration is with the vacancies at the edge of the nanowires. We also find that for multiple (two and three) nitrogen vacancies, the vacancies prefer to cluster together rather than remain well separated. For one and two gallium vacancies, the preferred vacancy location is also at the edge of the nanowires, with clustering favored for the two vacancies. Examining the band structure of unsaturated nanowires (with and without vacancies), we observe states in the band gap that can be attributed to edge states. These edge states are removed when the dangling bonds at the edge of the nanowires are saturated with hydrogen. For unsaturated wires, the nature of the single Ga and N vacancy states is similar to in the bulk, acting as a triple acceptor and single donor, respectively. The position of the vacancy states relative to the two regions of edge-induced states is similar to their location relative to the conduction band minimum and valence band maximum in the bulk, suggesting that any conductivity arising from the vacancies will be confined to the outer region of the nanowires. The two- and three-nitrogen vacancy complexes induce additional states in the band gap, acting as double and triple donors respectively, while the two-gallium vacancy complex reconstructs to an N_3-like structure and induces several fully occupied and unoccupied singlet state in the band gap. Examining the defect-induced states for the gallium vacancy in the saturated wire versus in bulk GaN, we find a similar result in terms of the number, location, and occupation of the defect states, except the states in the wire are slightly deeper in the band gap. For the nitrogen vacancy in the saturated wire versus in bulk GaN, we also find similar behavior in terms of the number and occupation of the defect states. However, the higher lying singly occupied state is closer to the conduction band in the wire, and the location of the fully occupied singlet state is below the valence band maximum in bulk GaN, and above it in the saturated nanowire. Considering the formation energy of gallium and nitrogen vacancies, we find nitrogen vacancies are significantly more stable than gallium vacancies, and thus we expect them to be the major defect in GaN nanowires.

DOI: 10.1103/PhysRevB.79.195302   PACS number(s): 73.22.−f, 73.61.Ey, 71.55.−i

I. INTRODUCTION

Nanotechnology is impacting almost all aspects of science and technology because of the unique properties of nanostructured materials, which result in potential uses in a wide range of areas from semiconductor devices to drug delivery systems.[1,2] Fundamental studies are required of these nanostructures to gain a more complete understanding of their special properties. Nanowires, in particular, represent important building blocks in nanotechnological applications. Gallium nitride (GaN) is a widely used III–V semiconductor in microelectronic and optoelectronic devices such as blue light-emitting diodes and lasers. GaN nanowires hold great promise for nanotechnology applications because of the large band gap and structural confinement properties and are being investigated for use in ultraviolet-blue light-emitting diodes, nanowire lasers, and potential spintronic devices.[3,4] Monocrystalline GaN nanowires have successfully been used as waveguides in an ultraviolet-blue laser.[5] For nanowires to be utilized to their full potential, we must improve our understanding of their properties and of the behavior of defects and of how these properties differ compared to the bulk. Native point defects, in particular, control many aspects of a semiconductor's function, so a detailed understanding of them is crucial.

The properties of bulk III-nitride compounds containing defects and dopants from first-principles calculations has been reviewed by Van de Walle and Neugebauer.[6] There have been numerous studies of defects in bulk GaN (Refs. 7–10); however to date, the structure, relative stability, and electronic properties of defects in gallium nitride *nanowires* has not been examined. In bulk GaN, nitrogen vacancies behave as shallow donors and gallium vacancies as acceptors.[6] Recent first-principles calculations by Ganchenkova and Nieminen[10] examined the positive and negative charge states for the nitrogen vacancy in bulk GaN and they found (for the first time) that the negative charge states are predicted to be stable and concluded that the nitrogen vacancy is the dominant defect in bulk GaN.

There have only been a few theoretical *ab initio* studies of the properties of GaN nanowires.[11–15] In our previous study,[15] we investigated GaN nanowires in the [0001] growth direction and examined the affect of their size and shape on the atomic and electronic properties. We found that dangling bonds at the edge of the nanowires induce edge states (ESs) in the band gap near the valence band maximum (VBM) and

    ©2009 The American Physical Society

conduction band minimum (CBM), while saturating these dangling bonds with hydrogen stabilizes these states and moves them out of the band gap.[15] We also found that the band gap of saturated wires decreases (essentially exponentially) with increasing wire diameter and approaches the band gap of bulk GaN, and further, that nanowires with a hexagonal-shaped cross section are more stable than those with a triangular-shaped cross section. Tsai *et al.*[13] examined unsaturated GaN [0001] nanowires and found that the average bond length of the nanowire decreases as the nanowire diameter decreases. Wang *et al.*[11,12] calculated the electronic structure of unsaturated GaN [0001] nanowires pair doped with manganese or chromium atoms and found that both dopants produce ferromagnetic coupling. Zhao *et al.*[16] examined both saturated and unsaturated AlN [0001] nanowires and found that nanowires with hexagonal-shaped cross sections are most stable and that the strain energy of unsaturated nanowires is inversely proportional to the nanowires diameter. To the best of our knowledge, there have been no *ab initio* studies of native defects in nanowires, in particular GaN, with the majority of studies instead focusing on the behavior of dopant atoms in the nanowires.

In the present paper, using first-principles calculations, we investigate the atomic and electronic properties of gallium and nitrogen vacancies in GaN nanowires and compare their behavior to that in bulk GaN. We also examine the stability of multiple vacancies to determine their preferred spatial distribution, for example, if there is a preference for clustering of defects. The influence of saturating the dangling bonds at the edge of the wires is also investigated. The paper is organized as follows. In Sec. II we describe the methodology we use for our density-functional theory (DFT) calculations, in Sec. III A we consider single (isolated) vacancies in bulk GaN as a reference for the nanowire investigations, and in Secs. III B and III C, we address single and multiple vacancies in GaN nanowires, respectively. In Sec. III D we discuss the influence on the electronic properties of saturating the dangling bonds at the edge of the wires with hydrogen and Sec. IV contains the conclusions.

II. METHODOLOGY

We perform DFT calculations using the SIESTA (Refs. 17 and 18) code, where we employ the generalized gradient approximation (GGA) of Perdew *et al.*[19] We use the norm-conserving pseudopotentials of Troullier and Martins,[20] with the valence electron configurations of gallium $3d^{10}$, $4s^2$, $4p^1$, nitrogen $2s^2$, $2p^3$, and hydrogen $1s^1$. A double zeta basis set with polarization functions is used for all atoms. The localized basis set in SIESTA consists of numerical atomic orbitals, which are radially confined to an extent that induces an energy shift in each orbital of 0.01 Ry. Hartree and exchange-correlation energies are evaluated on a uniform real-space grid of points with a defined maximum kinetic energy of 300 Ry. The Brillouin zone of wurtzite GaN bulk is sampled using an $(8\times8\times5)$ Monkhorst Pack[21] grid, generating 160 **k** points in the irreducible part of the Brillouin zone (IBZ). Using the optimised wurtzite GaN bulk structure, we generate a 96-atom $(3a\times2\sqrt{3}a\times2c)$ supercell (here a and c are the unit-cell dimensions of 3.28 and 5.31 Å, respectively) to examine vacancies in bulk GaN. A 96-atom supercell has been used in a number of previous studies of vacancies in bulk GaN,[6,9,22] with Ref. 6 reporting that absolute formations energies are sufficiently converged for this size supercell. We consider single gallium and nitrogen vacancies in the neutral charge state, and in the 1−, 2−, and 3− charge states for the gallium vacancy and in the 1+, 1−, 2−, and 3− charge states for the nitrogen vacancy. For these calculations, the Brillouin zone is sampled using a $(2\times2\times2)$ grid, producing four **k** points in the IBZ.

In our previous study[15] of GaN [0001] nanowires, we reported that nanowires with hexagonal-shaped cross sections are more stable than nanowires with triangular-shaped cross sections. For our vacancy studies, we therefore use nanowires in the [0001] growth direction with hexagonal-shaped cross sections that have diameters of 9.5 and 15.9 Å. In the [0001] direction, our simulation cells contain four GaN atomic layers. This produces a 96-atom (9.5 Å diameter) nanowire and a 216-atom (15.9 Å diameter) nanowire. In the planes normal to the nanowire growth direction, we use vacuum regions in our simulation cell, such that the separation between periodic images of nanowires is approximately 20 Å, to ensure that they do not interact. To determine the optimal location of the vacancies, we examine all possible sites for single gallium and nitrogen vacancies. To gain insight into the interaction between like vacancies, we also considered two and three nitrogen vacancies, as well as two gallium vacancies in the wires. These will be referred to as "two-vacancy" and "three-vacancy" configurations. The Brillouin zone for these calculations is sampled using a $(1\times1\times3)$ grid, generating two **k** points in the IBZ.

We calculate the formation energy[6] for a single vacancy (in the neutral or charged state) in bulk GaN using the equation,

$$E^f(V^q_{\mathrm{N(or\ Ga)}}) = E_{\mathrm{tot}}(V^q_{\mathrm{N(or\ Ga)}}) - E^{\mathrm{bulk}}_{\mathrm{tot}} + \mu_{\mathrm{N(or\ Ga)}} + q(E_{\mathrm{F}} + E_v + \Delta V), \quad (1)$$

where $E_{\mathrm{tot}}(V^q_{\mathrm{N(or\ Ga)}})$ is the total energy of the supercell containing the vacancy in charge state q, $E^{\mathrm{bulk}}_{\mathrm{tot}}$ is the total energy of the reference 96-atom GaN supercell, $\mu_{\mathrm{N(or\ Ga)}}$ is the chemical potential of the nitrogen (or gallium) atom, E_{F} is the Fermi level for the supercell with the vacancy, E_v is the energy of the bulk valence-band maximum, and ΔV is a correction term to align the reference potential in the defect with that in the bulk.

The formation energy for single or multiple gallium or nitrogen vacancies in GaN nanowires (in the neutral charge state) is calculated using the equation,

$$E^f = E^{\mathrm{wire}}_{V_{\mathrm{N(or\ Ga)}}} - E^{\mathrm{wire}}_{\mathrm{pure}} + x\mu_{\mathrm{N(or\ Ga)}}, \quad (2)$$

where $E^{\mathrm{wire}}_{V_{\mathrm{N(or\ Ga)}}}$ is the total energy of the nanowire with the nitrogen (or gallium) vacancies, $E^{\mathrm{wire}}_{\mathrm{pure}}$ is the total energy of the nanowire with no vacancies, and x is the number of vacancies. We primarily report formation energies using gallium-rich conditions, where μ_{Ga} is the energy of a gallium atom in bulk α-gallium. The nitrogen chemical potential μ_{N}

is then determined using the assumption of thermodynamic equilibrium $\mu_{Ga}+\mu_{N}=\mu_{GaN}$, where μ_{GaN} is the chemical potential of bulk GaN. Under nitrogen-rich conditions, μ_N is the energy of a nitrogen atom in a nitrogen molecule and μ_{Ga} is then determined using the above-mentioned assumption of thermodynamic equilibrium. For nitrogen-rich conditions, the formation energies of single gallium and nitrogen vacancies are shifted by −0.92 and +0.92 eV, respectively (corresponding to ΔH_f and $-\Delta H_f$, where ΔH_f is the heat of formation of GaN), with respect to the values under gallium-rich conditions. ΔH_f is calculated by the expression $\Delta H_f(\mathrm{GaN}) = \mu_{GaN} - \mu_{Ga} - \frac{1}{2}\mu_{N_2}$, where μ_{GaN} is the total energy of bulk GaN, μ_{Ga} is the total energy of a gallium atom in bulk α-gallium and μ_{N_2} is the total energy of a nitrogen molecule. For nitrogen-rich conditions, the total formation energies of two gallium and two nitrogen vacancies are shifted by −1.84 and +1.84 eV, respectively (corresponding to $2\times\Delta H_f$ and $-2\times\Delta H_f$) and for three nitrogen vacancies, the total formation energy is shifted by +2.76 eV (corresponding to $-3\times\Delta H_f$), with respect to the values under gallium-rich conditions.

III. RESULTS & DISCUSSION

A. Single Ga and N vacancies in bulk GaN

Before examining vacancies in GaN nanowires, we first examine single Ga and N vacancies in the 96-atom bulk GaN supercell and compare to other *ab initio* calculations. These results will be used as a reference with which to compare the behavior of the vacancies in the nanowires. The optimized bulk wurtzite GaN lattice constants are a=3.28 Å, c=5.31 Å, and u=0.378, which compare well with—but slightly overestimate—the experimental values of a=3.19 Å, c=5.19 Å, and u=0.377.[23] The band gap is 1.44 eV, noticeably underestimated compared to the experimental band gap of 3.50 eV,[24] however this is a well-understood phenomena of band gaps calculated using DFT. We reported the band structure, heat of formation, bulk modulus, and cohesive energy of bulk GaN in our earlier publication,[15] to which we refer for further details.

For a single gallium vacancy, in the neutral charge state, the neighboring nitrogen atoms are displaced outward from the vacancy, with the Ga-N bond lengths of these neighboring atoms contracting by 2.9–3.7 %, with respect to the Ga-N bond length in the bulk. This is in good agreement with the 3.5–3.7 % contraction reported by Neugebauer and Van de Walle[7] using the plane-wave pseudopotential method with the local-density approximation (LDA) and explicitly including the 3d electrons for gallium. We plot the band structures for the neutral gallium (V_{Ga}) and nitrogen (V_N) vacancies in Figs. 1(a) and 1(b), respectively, and also provide a schematic illustration of the defect-induced electronic states in Fig. 1(c). To determine which states belong to the defect or the bulk, we investigate the spatial distribution of the corresponding wave functions at the Γ point.

For the neutral charge state of the nitrogen vacancy, we find that neighboring gallium atoms are displaced outward from the vacancy, with the Ga-N bond lengths of these

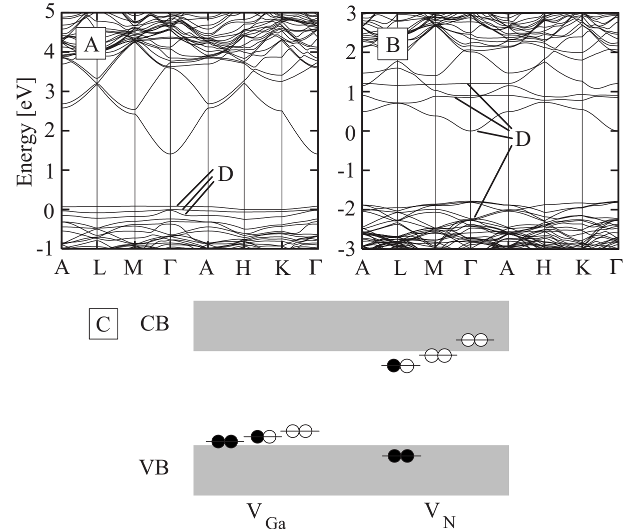

FIG. 1. Band structure of the 96-atom wurtzite GaN supercell, containing a single (a) gallium and (b) nitrogen vacancy, in the neutral charge state. The energy zero is set at the highest occupied state and defect states are labeled with a "D." (c) Corresponding schematic representation of the defect-induced levels, where filled and open circles denote electrons and holes, respectively. "CB" and "VB" represent the conduction band and valence band, respectively.

neighboring atoms contracting by 0.2–0.3 %, with respect to the bond lengths in the bulk. These values are somewhat smaller than the 3.7–3.9 % contraction reported in DFT-GGA calculations by Gulans *et al.*,[22] using a linear combination of Gaussian atomic orbitals method or the ~5% contraction reported by Neugebauer and Van de Walle[25] using the plane-wave pseudopotential DFT-LDA method. Neither of these authors[22,25] included the 3d electrons for gallium but rather used nonlinear core corrections (NLCCs), which may explain why we observe a smaller contraction.

For the gallium vacancy, we find three singlet states [see Fig. 1(c)] located close to but above (0.2, 0.25, and 0.3 eV above) the VBM, with the lowest of the singlet states fully occupied, the second lowest singlet containing one electron, and the highest singlet state unoccupied. Thus, we consider the 1−, 2−, and 3− charge states. Neugebauer and Van de Walle[7,25] reported that the gallium vacancy in GaN, from DFT-LDA calculations, has a doublet and singlet state located just above the VBM, where the lower lying doublet is occupied by three electrons and the singlet state is unoccupied. This compares well with our results, except that we do not obtain an induced doublet defect state but rather two singlet states near the VBM.

For the nitrogen vacancy, we find four defect-induced singlet states [see Fig. 1(c)], with one singlet state fully occupied, 0.5 eV below the VBM, and three states near the CBM. For the states near the CBM, we find that two are below the CBM (0.1 and 0.9 eV below), with the lower of these two occupied by one electron and the higher state unoccupied. The remaining singlet state is located 0.3 eV above the CBM and is unoccupied. We therefore consider the 1+ charge state and also the 1−, 2−, and 3− charge states. Neugebauer and Van de Walle[7,25] reported that the nitrogen vacancy induces a fully occupied singlet state below the VBM and a singlet and

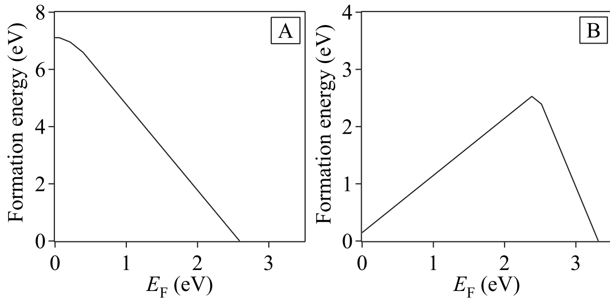

FIG. 2. Formation energies of a (a) gallium and (b) nitrogen vacancy in various charge states as a function of the Fermi level (E_F). The zero of the Fermi level corresponds to the top of the valence band and we show the Fermi energy spanning the experimental band gap. The results for gallium-rich conditions are shown, and the slopes of each line indicate the charge state. We only show the most favorable charge state at a particular value of the Fermi level. A change in slope of the line corresponds to a transition between charge states. For the (a) gallium vacancy, the neutral, 1−, 2−, and 3− charge states are shown, and for the (b) nitrogen vacancy, the 1+, 1−, and 3− charge states are shown.

a doublet state above the CBM, with the singlet state occupied by one electron. This compares qualitatively with our results, except that—as found for the gallium vacancy—we observe two singlets rather than a doublet, and we find two of the singlet states are below the CBM. Group theory suggests that for wurtzite GaN, we should observe a doublet and a singlet state. However, we find that all the Ga-N bonds around the vacancy are not identical after relaxation (the SIESTA code does not use symmetry constraints), leading to the splitting of the doublet into two singlet states.

We next investigate charged Ga vacancies. For the 1−, 2−, and 3− charge states, the neighboring nitrogen atoms displace outward from the vacancy, with the Ga-N bond lengths of these atoms contracting by 3.1–3.8 %, 4.2–4.8 %, and 5.3–6.0 %, respectively, compared to 2.9–3.7 % for the neutral charge state. The values of the relaxations in the literature are quite varied, with DFT-LDA calculations of Neugebauer and Van de Walle[7] reporting a 3.5–6.0 % contraction for the 0, 1−, 2−, and 3− charge states, in good agreement with the present values. Limpijumnong and Van de Walle[9] reported an ~4% contraction and Ganchenkova and Nieminen[10] reported an ~8% contraction. Even larger values of 10–12 % have also been reported.[26] These differences may be caused by the choice of basis set and the description of the gallium 3*d* electrons; for example, DFT-LDA methods using a projector augmented wave (PAW) basis set,[10] DFT-LDA pseudopotential plane-wave methods using the NLCC (Ref. 9) to describe the Ga 3*d* electrons or including Ga 3*d* electrons as valence electrons,[7,26] and the DFT-GGA local-orbital approach with Ga 3*d* electrons included as valence electrons that we use in the present study.

We plot the formation energy versus Fermi level for the gallium vacancy in Fig. 2(a), for gallium-rich conditions. In Fig. 2 we only show the most stable charge state for a particular value of the Fermi level value (rather than showing all lines), and the charge state can be determined from the slope of the line at any particular point. We find a transition from the neutral charge state being most stable to the higher charge states being most stable, as the Fermi level increases. These transitions are (0/1−), (1−/2−), and (2−/3−) charge states and are located at 0.1, 0.2, and 0.4 eV above the VBM, respectively. This agrees qualitatively well with the results of other studies. However, the Fermi level values for the transitions are more spread in these other studies; e.g., Limpijumnong and Van de Walle[9] reported values of 0.2, 0.7, and 1.1 eV, Ganchenkova and Nieminen[10] reported values of 0.4, 0.8, and 1.1 eV, Mattila and Nieminen[27] reported values of 0.5, 1.0, and 1.5 eV, and Neugebauer and Van de Walle[7] reported values of 0.4, 1.0, and 1.9 eV, for the same transitions. We also repeated these calculations[28] using the DFT-GGA method in the $DMol^3$ code[29,30] and found these transitions to be 0.2, 0.6, and 1.1 eV. The location of the transitions is sensitive to the value of the band gap and band gaps are very sensitive to the choice of basis set, leading to a variation in band gaps reported for bulk GaN. In the present SIESTA calculations, we use DFT-GGA with a numerical orbital basis set and Troullier and Martins[20] pseudopotentials and find a band gap of 1.44 eV. Plane-wave DFT-GGA calculations with the same pseudopotentials by Stampfl and Van de Walle[31] reported a similar band gap of 1.45 eV. When we used the DFT-GGA method within the $DMol^3$ code, with a numerical orbital basis set and semilocal density-functional semicore pseudopotentials (DSPPs),[32] we found a band gap of 2.58 eV.[28] Plane-wave DFT-LDA calculations report bands gaps of 1.8 eV (Ga 3*d* included as valence),[31] 1.9 eV (Ga 3*d* included as valence),[33] and 2.7 eV (Ga 3*d* described using the NLCC). It is well known that using the NLCC leads to a larger band gap.[27] The smaller band gap in our present calculations forces these transitions to be more compressed and thus occur across a smaller range of the Fermi level.

We now consider charged N vacancies. For the nitrogen vacancy with a 1+ charge state, we find that the neighboring gallium atoms are displaced outward from the vacancy, with the Ga-N bond lengths of these atoms contracting by 0.5–0.8 %, compared to the 0.2–0.3 % contraction obtained for the neutral charge state. This compares well with DFT-LDA calculations for the 1+ charge state reported by Neugebauer and Van de Walle,[7] with outward relaxations of 0.5–1.5 % for a 32-atom supercell and 0.5–1.6 % (Ref. 9) for a 96-atom supercell. For the 1−, 2−, and 3− charge states, we find that the neighboring gallium atoms are displaced inward toward the vacancy, with the Ga-N bond lengths of these atoms expanded by 0.1–0.3 %, 0.7–2.9 %, and 3.1–6.3 %, respectively. It should be noted that only recently the negative charge states for the nitrogen vacancy V_N in GaN were considered. In particular, Ganchenkova and Nieminen[10] found that the 1−, 2−, and 3− charge states were stable, making V_N the lowest-energy native defect. They also observed that neighboring gallium atoms were displaced inward toward the vacancy for the negative charge state vacancies, resulting in Ga-N bond lengths of these neighboring atoms expanding. They reported that the amount of expansion increases with the charge state, such that it is 10.2% for the 3− charge state. This trend is qualitatively the same as the present results, although the latter expansion is somewhat greater.

We plot the formation energy versus Fermi level for the nitrogen vacancy in Fig. 2(b), for gallium-rich conditions. We find the 1+, 1−, and 3− charge states are stable, with transitions of (1+/1−) and (1−/3−) located at 2.40 and 2.50 eV above the VBM, respectively. It should be noted that although the CBM is 1.44 eV above the VBM, which indicated these transitions occur above the CBM, we have verified by plotting the spatial distributions of the wave functions at the Γ point that these levels that we occupy with 1, 2, and 3 electrons are really defect related states.

Ganchenkova and Nieminen[10] reported that the 1+, 1−, 2−, and 3− are all stable, with transitions of (1+/1−), (1−/2−), and (2−/3−) located at 2.43, 2.58, and 2.60 eV above the VBM, respectively. Our results agree qualitatively with these results, except that Ref. 10 finds that the 2− charge state is stable, but only in a very small energy range (0.02 eV) of the Fermi level.

It should be noted that there is some discrepancy in the literature over the existence of the 3+ charge state for the nitrogen vacancy. The 3+ charge state has been reported to be stable in pseudopotential plane-wave DFT-LDA calculations by Van de Walle and co-workers,[9,34] using the NLCC for the gallium 3*d* electrons. On the other hand, the 3+ charge state has been reported to *not* be stable in DFT-LDA calculations by Mattila and Nieminen,[27,35] using a pseudopotential plane-wave method with NLCC for the gallium 3*d* electrons, and by Ganchenkova and Nieminen,[10] using the projected augmented wave method, and also in the present work. When the 3+ charge state of the nitrogen vacancy is reported as stable, the neighboring gallium atoms are displaced outward from the vacancy, with the Ga-N bond lengths of these neighboring atoms reported to have large contractions of 16–20 % (Ref. 8) and 16.6–18.1 %.[9] Van de Walle and Neugebauer[6] suggested that the large contractions allow the fully occupied singlet state, which is located below the VBM for the neutral charge state, to move above the VBM, thus allowing the existence of the 3+ charge state. Limpijumnong and Van de Walle[9] suggested that the use of a larger supercell (96-atom) allows for a better relaxation of the 3+ charge state vacancy, adding to the stability, which is why it was not observed in their earlier work[7] using a 32-atom supercell. Neugebauer and Van de Walle[7] and Mattila and Nieminen[27,35] used 32-atom supercells, so this argument may be valid in reference to these papers. However, we use a 96-atom supercell and Ganchenkova and Nieminen[10] used an even larger 300-atom supercell, and neither studies find that the 3+ charge state is stable. The differing behavior may instead be attributed to the different numerical codes rather than the size of the supercell and warrants further investigations, also for the nitrogen vacancy in AlN and InN.

B. Single Ga and N vacancies in GaN nanowires

For studying the vacancies in the nanowires, we use 96-atom (9.5 Å diameter) and 216-atom (15.9 Å diameter) wires with hexagonal-shaped cross sections (see Fig. 3), in which the periodicity of the wires along the *c* axis is doubled. As mentioned earlier, for saturated wires with increasing diameter, the band gap decreases, approaching the bulk GaN value, while for unsaturated wires, it remains rather constant. In particular, the effective band gaps for the unsaturated 96- and 216-atom wires are 1.24 and 1.25 eV, respectively (i.e., very similar), and for the saturated 96- and 216-atom wires the band gaps are 3.23 and 2.45 eV, respectively. Clearly, due to the well-known underestimate of DFT-GGA(LDA) band gaps, in reality these values would be notably larger. In Fig. 4, for saturated nanowires, we show the VBM and CBM as a function of increasing nanowire diameter, for wires with both hexagonal- and triangular-shaped cross sections. It can be seen that the CBM exhibits a greater variation than the VBM over the nanowire size range examined. In particular, as the diameter of hexagonal-shaped cross section nanowires varies from 9.5 to 35.0 Å, the shifts of the VBM and CBM are +0.30 and −1.1 eV, respectively. Similarly, for nanowires with triangular-shaped cross sections that vary from 6.4 to 25.4 Å, the shifts of the VBM and CBM are +0.47 and −1.46 eV, respectively.

For Si nanowires in the [011] growth direction with diameters ranging from 12 to 22 nm, Wu *et al.*[36] found that the shifts of the VBM and CBM for nanowires with straight sides are +0.31 and −0.34 eV, respectively, while for nanowires with tapered sides, the shifts are −0.1 and −0.6 eV, respectively. From these results, they suggest that for small-diameter-tapered Si nanowires, the eigenstates in the conduction band are much more sensitive to the diameter than those

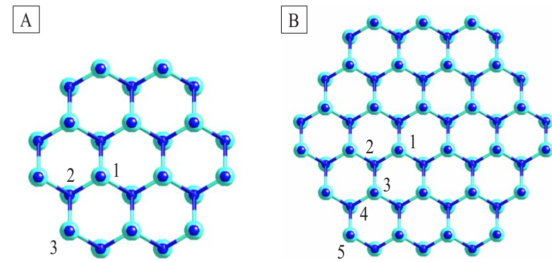

FIG. 3. (Color online) Illustration of the (a) 96-atom and (b) 216-atom nanowires viewed along the [0001] direction (i.e., showing the cross section). The possible locations for a gallium or nitrogen vacancy are numbered for each nanowire. Nitrogen and gallium atoms are indicated by the small dark (blue) and large light (aqua) spheres, respectively.

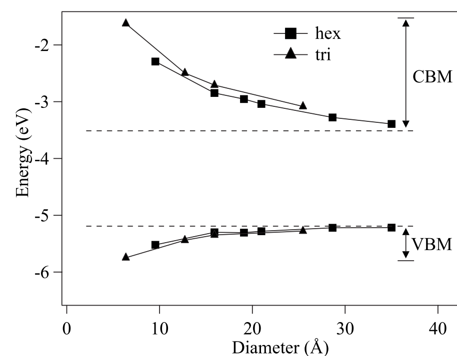

FIG. 4. VBM and CBM values as a function of nanowire diameter for saturated GaN nanowires with hexagonal and triangular-shaped cross sections. "Hex" and "tri" refer to nanowires with hexagonal- and triangular-shaped cross sections, respectively.

TABLE I. Formation energies (eV) of single Ga and N vacancies in the 96- and 216-atom nanowires. Formation energies are given relative to the formation energy of the most stable site (see Fig. 3) for the particular nanowire size and type of vacancy.

Site	96-atom		216-atom	
	V_{Ga}	V_N	V_{Ga}	V_N
1	0.3	1.3	1.2	1.6
2	1.0	1.1	1.1	1.5
3	0.0	0.0	0.4	1.2
4			1.3	1.1
5			0.0	0.0

states in the valence band. From the results in Fig. 4, we also find this behavior for GaN nanowires, over the size range we examined.

We first examine single gallium and nitrogen vacancies in the 96-atom (9.5 Å diameter) and 216-atom (15.9 Å diameter) unsaturated nanowires to determine the most stable configurations and the influence of the nanowire diameter. We define the nanowire diameter as the maximum distance between edge atoms on opposite sides of the nanowire. The possible vacancy locations considered are shown in Fig. 3. We calculate the formation energies [cf. Eq. (2)], for gallium-rich conditions. The relative formation energies are listed in Table I. For both the 96- and 216-atom nanowires, the most stable gallium and nitrogen vacancy sites are located at the edge of the nanowire [site number 3 in Fig. 3(a) and site number 5 in Fig. 3(b) for the 96- and 216-atom wires, respectively]. The formation energies for the most stable configurations for the nitrogen vacancy in both the "small" and "large" wires are 1.1 eV more stable than the next most stable configuration [site number 2 in Fig. 3(a) and site number 4 in Fig. 3(b) for the 96- and 216-atom wires, respectively]. For the gallium vacancy, we find that the most stable configurations are 0.3–0.4 eV more stable than the next most stable configuration [site number 1 in Fig. 3(a) and site number 3 in Fig. 3(b) for the 96- and 216-atom wires, respectively]. For the most stable Ga and N vacancies, we performed spin-polarized calculations and find they are magnetic resulting in an energy lowering of 0.7 and 0.14 eV, respectively.

The formation energies for the nitrogen vacancy in the 96-atom nanowire are in the range of +0.7–+2.0 eV and +0.6–+2.2 eV for the 216-atom nanowire. For a gallium vacancy, the formation energies in the 96-atom nanowire are in the range of +4.5–+5.5 eV and +5.9–+7.1 eV for the 216-atom nanowire. For the neutral charge states, nitrogen vacancies are significantly more stable (i.e., lower in energy) than gallium vacancies. This situation may be different for charged vacancies, however we do not address this because there is not a valid charge compensation scheme in SIESTA for treating charged nanowires in a supercell.

We now examine in more detail the formation energies for a nitrogen vacancy and examine if it exhibits a size effect for the 96-atom and 216-atom nanowires. Looking at the formation energies of the most stable configurations in the 96-atom and 216-atom wires, there is no significant difference (0.7 and 0.6 eV, respectively). To investigate a size effect, we also examine vacancies in the center of the nanowires and compare to results for vacancies in the bulk. If the nanowire diameter is infinitely large, the formation energy of the vacancy at the center of the nanowire should be the same as for a single nitrogen vacancy in bulk GaN, i.e., 2.5 eV. For the most stable nitrogen vacancies at the center of the 96-atom and 216-atom nanowires, the formation energies are 2.0 and 2.2 eV, respectively. Thus, displaying a small size effect. The significantly lower formation energies of the nitrogen vacancies at the edges of nanowires indicate that this defect may be more abundant in the nanowires compared to in bulk GaN.

We now investigate size effects for the gallium vacancies in the 96- and 216-atom nanowires. Looking at the formation energies of the most stable configurations, in the 96-atom wire it is +1.4 eV more favorable (lower in energy) than in the 216-atom wire, indicating a notable size effect. If the nanowire diameter is infinitely large, the formation energy of the vacancy at the center of the nanowire should be the same as for a single gallium vacancy in bulk GaN, i.e., 7.1 eV. For the most stable gallium vacancies at the center of the 96-atom and 216-atom nanowires, the formation energies are 5.6 and 7.1 eV, respectively, also indicating a significant size effect, particularly for the 96-atom nanowire. In the smaller 96-atom wire, there is less "bulk-like" GaN in the center of the wire (because of the smaller diameter), which allows greater freedom for relaxation around the vacancy, leading to a more favorable formation energy. This affect was not significant for the nitrogen vacancy and can be explained by the magnitudes of the atomic relaxations around the vacancies. As discussed in Sec. III A for bulk GaN, the Ga-N bond lengths of neighboring atoms around nitrogen vacancies contract by a small amount of 0.2–0.3 %, while around gallium vacancies, the contraction is larger with values of 2.9–3.7 %. A similar behavior is also observed for vacancies in the nanowires, with much larger bond length changes around the gallium vacancies, discussed in more detail later in this section. So the larger atomic relaxations around gallium vacancies lead to the observation of a size effect, in particular, for the 96-atom nanowire.

Examining in more detail the geometries of the most stable nitrogen vacancy configurations, for the 96-atom nanowire the neighboring gallium atoms are displaced inward toward the vacancy, with the Ga-N bond lengths of these atoms expand by 0.3–3.6 %, with respect to the bond lengths in the relaxed wires with no vacancies. In the 216-atom wire, there is an expansion of Ga-N bond lengths by 0.2–2.6 %. This is in contrast to the nitrogen vacancy in bulk GaN, where there is a small contraction of Ga-N bond lengths of neighboring atoms of 0.2–0.3 %. This variation can be attributed to the different locations and atomic environments of the vacancy at the edge of the nanowire compared to the vacancy in bulk GaN. The vacancy configuration at the edge of the nanowire has one neighboring gallium atom missing, in comparison to the vacancy in bulk, which allows greater freedom for movement of atoms, and thus larger atomic relaxations.

The single nitrogen vacancy induces several defect states below the ES region near the CBM, as illustrated in the band

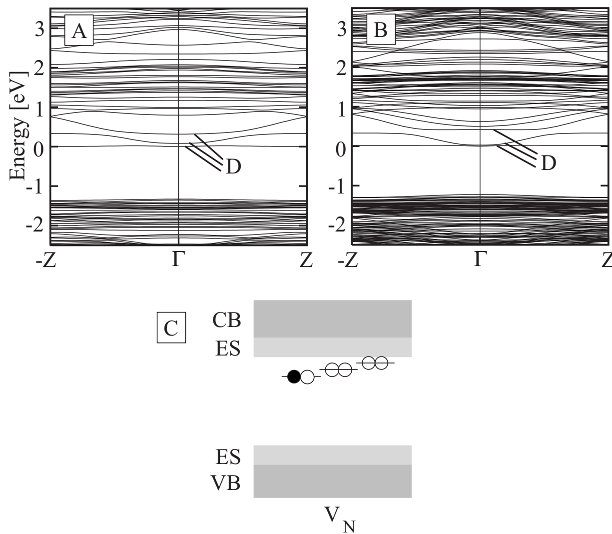

FIG. 5. Band structure of the most stable configurations for the single nitrogen vacancy in the (a) 96-atom and (b) 216-atom nanowires. The energy zero is set at the highest occupied state and defect states are labeled with a "D." (c) Corresponding schematic representations of the defect-induced levels for both size nanowires, where filled and open circles denote electrons and holes, respectively. "CB," "VB," and "ES" represent the conduction band, valence band, and edge states, respectively.

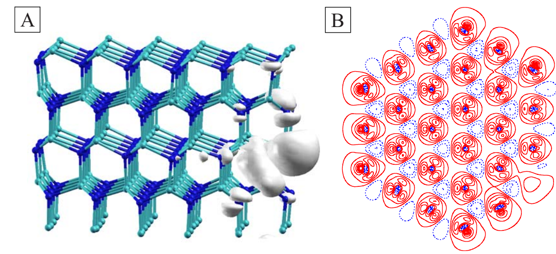

FIG. 6. (Color online) (a) The spatial distribution of the singly occupied defect state [see Fig. 5(c)] at the Γ point for the single nitrogen vacancy in the 216-atom nanowire. Nitrogen and gallium atoms are indicated by dark (blue) and light (aqua) spheres, respectively, and the orbitals are pale gray. (b) The difference electron-density distribution in the plane of the vacancy for the single nitrogen vacancy in the 216-atom nanowire. Solid (red) lines indicate charge accumulation and dashed (blue) lines indicate charge depletion.

structure in Figs. 5(a) and 5(b) for the 96-atom and 216-atom nanowires, respectively. We investigate the spatial distribution of the corresponding wave functions at the Γ point to determine which states belong to the defect, the bulk or the edge states. There are three singlet states just below the top of the ES region near the CBM, with the lowest of these states occupied by one electron, while the other two defect states remain unoccupied. This is illustrated schematically in Fig. 5(c). Comparing this to the single nitrogen vacancy in the 96-atom bulk (Sec. III A), we find that there is one less singlet state for a vacancy in the nanowires, i.e., no fully occupied singlet state below the VBM (or just below the top of the ES region). We also find a slight difference in the location of the defect-induced states in the region of the CBM, with bulk calculations finding two of the singlet states just below the CBM (0.1 and 0.9 eV below) and one singlet state 0.3 eV above the CBM; whereas for the nanowires, the three singlet states are all just below the top of the ES region near the CBM. For the 96-atom nanowire the three singlet states are located 0.5, 0.7, and 0.8 eV below the top of the ES region near the CBM, while for the 216-atom nanowire, they are located 0.1, 0.45, and 0.5 eV below, respectively. Thus, the defect states are slightly closer to the ES region near the CBM in the larger nanowire. In Fig. 6(a) we show the spatial distribution of the occupied defect state at the Γ point, where it can be seen that it is localized in the region of the vacancy. Figure 6(b) shows (in the plane of the vacancy) the difference electron-density distribution, which is the difference between the total electron density of the wire and the superimposed sum of atomic densities of the Ga and N atoms in the positons they have in the wire. The increase in electron density at the vacancy site can be clearly seen.

We now examine in more detail the geometries of the most stable gallium vacancy configurations. For the 96-atom nanowire, we find that the neighboring nitrogen atoms are displaced outward from the vacancy, with the Ga-N bond lengths of these neighboring atoms contracting by 1.4–7.6 %, with respect to the bond lengths in the relaxed wires with no vacancies. In the 216-atom nanowire, this contraction is 1.0–5.3 %. In the 96-atom bulk GaN, we also found a contraction in the Ga-N bond lengths of neighboring nitrogen atoms, with values of 2.9–3.7 % for the neutral charge state. The relaxations are larger when the vacancies are located at the edges of nanowires because they are missing a nearest-neighbor atom (compared to bulk GaN), which allows more room for relaxations to occur around the vacancy.

The band structures for a single gallium vacancy in the 96-atom and 216-atom nanowires are shown in Figs. 7(a) and 7(b), respectively. To determine which states belong to the defect, the bulk, or the edge states, we again investigate the spatial distribution of the corresponding wave functions at the Γ point. The induced defect states are shown schematically in Fig. 7(c). We find two defect-induced states just above the ES region near the VBM, with the lower of these two states occupied by one electron, while the higher of the two remains unoccupied. As discussed in Sec. III A, for a gallium vacancy in the bulk, we find three singlet states 0.2, 0.25, and 0.3 eV above the VBM. Thus, for the wires there is one less singlet state present in the band gap, namely, the lowest lying fully occupied singlet state. For the 96-atom nanowire, the two singlet states are located at 0.2 and 0.3 eV above the ES region near the VBM, while for the 216-atom nanowire, they are 0.1 and 0.2 eV above, respectively. In Fig. 8(a) we show the spatial distribution of the occupied defect state at the Γ point, where it can be seen that it is localized in the region of the vacancy. Figure 8(b) illustrates (in the plane of the vacancy) the difference electron-density distribution which clearly shows an increase in the electron density at the vacancy site.

C. Multiple Ga and N vacancies in GaN nanowires

Having investigated the behavior of single Ga and N vacancies in GaN nanowires, we now consider multiple vacan-

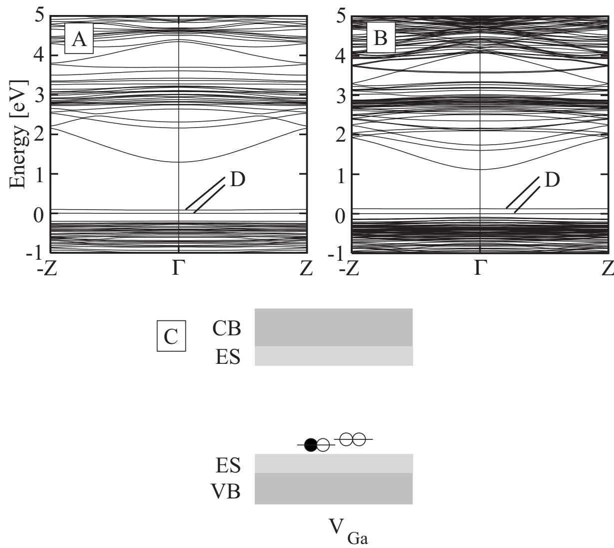

FIG. 7. Band structure of the most stable configurations for the single gallium vacancy in the (a) 96-atom and (b) 216-atom nanowires. The energy zero is set at the highest occupied state and defect states are labeled with a "D." (c) Corresponding schematic representations of the defect-induced levels for both size nanowires, where filled and open circles denote electrons and holes, respectively. "CB," "VB," and "ES" represent the conduction band, valence band, and edge states, respectively.

cies and determine the preferred spatial distribution. We examine nitrogen two-vacancy and three-vacancy configurations and gallium two-vacancy configurations in the 216-atom (15.9 Å diameter) unsaturated nanowire.

1. Multiple N vacancies

To determine the energetically most favorable configuration of nitrogen vacancies, we investigate 50 different two-vacancy configurations and 20 different three-vacancy configurations in the 216-atom nanowire. The most stable two-vacancy and three-vacancy configurations are illustrated in Figs. 9(a) and 9(b), respectively. The total formation energies for the two-vacancy and three-vacancy configurations are in

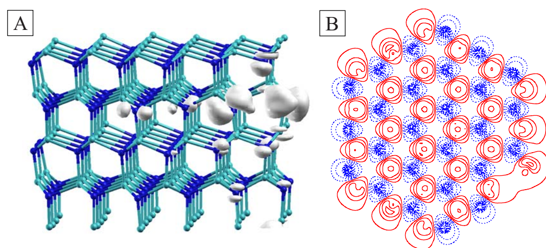

FIG. 8. (Color online) (a) The spatial distribution of the singly occupied defect state [see Fig. 7(c)] at the Γ point for the single gallium vacancy in the 216-atom nanowire. Nitrogen and gallium atoms are indicated by dark (blue) and light (aqua) spheres, respectively, and the orbitals are pale gray. (b) The difference electron-density distribution in the plane of the vacancy for the single gallium vacancy in the 216-atom nanowire. Solid (red) lines indicate charge accumulation and dashed (blue) lines indicate charge depletion.

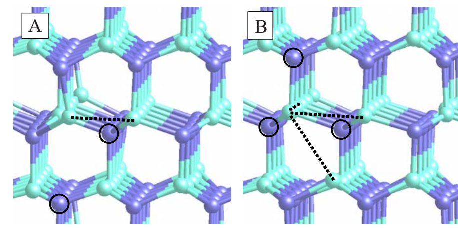

FIG. 9. (Color online) The most stable nitrogen (a) two-vacancy and (b) three-vacancy configurations in the 216-atom nanowire. Nitrogen and gallium atoms are indicated by the dark (blue) and light (aqua) spheres, respectively. The dashed line in (a) indicates the reduced gallium-gallium separation distance of 2.65 Å (compared to 3.28 Å in bulk GaN). The three dashed lines in (b) indicate the reduced gallium-gallium separation distances of 3.03, 3.08, and 3.11 Å. The open circles represent the location of the missing nitrogen atoms.

the range of $-0.4-+4.4$ eV ($-0.2-+2.2$ eV per vacancy) and $-0.2-+5.6$ eV ($-0.07-+1.87$ eV per vacancy), respectively, under gallium-rich conditions. The negative energies of the most favored configurations indicate that they are more stable than the unsaturated reference wires. Reasons for this are suggested below. As mentioned in Sec. II, under nitrogen-rich conditions, the total formation energies for the nitrogen two-vacancy and three-vacancy configurations are larger by $+1.84$ eV$(-2\times\Delta H_f)$ and $+2.76$ eV$(-3\times\Delta H_f)$, respectively, thus making all the values positive. For the most stable two- and three-vacancy configurations, we carried out spin-polarized calculations and found a very small magnetism and associated lowering of the total formation energy of 0.01 and 0.10 eV, respectively.

We first examine the formation energy per vacancy for single and multiple nitrogen vacancies at the center of the 216-atom nanowire to see how this compares to a nitrogen vacancy in the bulk. In bulk GaN, the formation energy of the nitrogen vacancy is 2.5 eV. The formation energy per vacancy, for nitrogen vacancies (on nearest-neighbor sites) at the center of the 216-atom nanowire, is 2.1, 1.6, and 1.0 eV, for one-, two-, and three-vacancy configurations, respectively. The formation energy per vacancy thus decreases as the number of vacancies increases, suggesting an attractive interaction between the nitrogen vacancies. We find an attractive interaction between vacancies at the edge of the wires as described below, which is their favored location.

The most stable two-vacancy configuration has both vacancies at the edge of the nanowire, with the vacancies as close as possible to each other, but in different nitrogen (0001) planes, which we refer to as "out-of-plane." The total formation energy of the most stable configuration is 1.0 eV more favorable than the next most favorable configuration, which also has the vacancies at the edge of the nanowire, but "in-plane" [same nitrogen (0001) plane] with each other, and as close as possible to each other, i.e., nearest-neighbor (like-species) sites. When the two vacancies are well separated—but still at the edge of the nanowire—the configuration is 1.8 eV less stable than the most favorable configuration, showing that the vacancies prefer to be clustered. When the two nitrogen vacancies are at the center of the nanowire, the configuration is 4.2 eV less stable than the most favorable struc-

ture, demonstrating that the vacancies prefer to be at the edge of nanowires (as also found for the single nitrogen vacancy). To understand the difference in stability of the in-plane and out-of-plane vacancy configurations, we examine in more detail the geometries of the configurations.

For the most stable two-vacancy configuration, with the out-of-plane vacancy configuration [Fig. 9(a)], we find a reduced separation between two gallium atoms around the vacancy, with a distance of 2.65 Å. This separation is noticeably smaller than the Ga-Ga separation of 3.28 Å we find in bulk GaN and more similar to the Ga-Ga separation of 2.55 Å we find in bulk α-Ga. Examining the Ga-N bond lengths for the gallium atoms involved with the reduced separation distance, we find that they are slightly expanded by 1.5–1.9 %, with respect to the bond lengths in the relaxed wire with no vacancies. For other gallium atoms surrounding the nitrogen vacancies, the Ga-N bond lengths for these atoms are also expanded by 1.0–4.1 %. To investigate the difference in the stability of the in-plane and out-of-plane vacancy configurations at the edge of the nanowires, we again examine the gallium atom separation around the vacancies. For the out-of-plane configuration, the closest separation is 2.65 Å, while for the in-plane configuration, the closest separation is 2.76 Å. Thus, one factor making the out-of-plane configuration more favorable is that it allows a greater relaxation of gallium atoms.

We now examine the most stable nitrogen three-vacancy configuration. In this configuration, all vacancies are located at the edge of the nanowires and are clustered together. The geometry is similar to the most stable configuration for two nitrogen vacancies, with two of the vacancies out-of-plane to each other (different nitrogen (0001) planes), while the third nitrogen vacancy is in-plane with one of the vacancies—again all situated as close as possible to each other. Examining the total formation energies, the most stable three-vacancy configuration is 0.4 eV more favorable than the next most favorable configuration, which has the vacancies at the edge of the nanowire but all in-plane [same nitrogen (0001) plane] with each other and on nearest-neighbor (like-species) sites. When the three nitrogen vacancies are well separated—but still at the edge of the nanowire—the configuration is 2.2 eV less stable than the most favorable configuration and when the vacancies are at the center of the nanowire, the configuration is 3.2 eV less stable than the most favored one. This again shows that the vacancies have an attractive interaction and prefer to be clustered together rather than well separated and that they prefer to be at the edge of nanowires rather than in the bulk. Such a clustering behavior of multiple nitrogen vacancies has been found in bulk InN,[37] AlN,[38] and GaN.[38]

When we examine the atomic geometries of the most favorable three-vacancy configuration [Fig. 9(b)], we find Ga-Ga in-plane separation distances of 3.08 and 3.11 Å and an out-of-plane separation of 3.03 Å. As mentioned above, in the relaxed pure nanowire, the Ga-Ga separations in-plane are ~3.27 Å. Therefore, as found for the two-vacancy configuration, we observe a reduced Ga-Ga separation around the vacancies. For other gallium atoms surrounding the nitrogen vacancies, the Ga-N bond lengths of these atoms are expanded by 0.3–2.6 %.

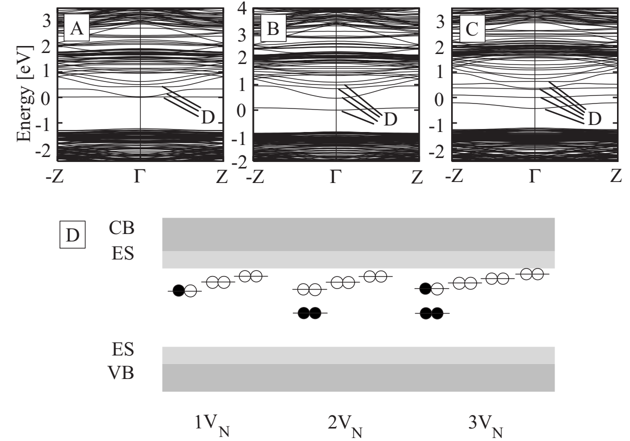

FIG. 10. The band structure of the most stable nitrogen (a) single vacancy and (b) two- and (c) three-vacancy configurations in the 216-atoms nanowire. The energy zero is set at the highest occupied state and defect states are labeled with a "D." (d) Corresponding schematic representation of the defect-induced levels for one, two, and three nitrogen vacancies, where filled and open circles denote electrons and holes, respectively. "CB," "VB," and "ES" represent the conduction band, valence band, and edge states, respectively.

The band structures of the most stable two-vacancy and three-vacancy configurations are shown in Figs. 10(b) and 10(c), respectively [that of the most stable single vacancy configuration is also shown in Fig. 10(a) for comparison]. To determine which states belong to the defect, the bulk or the edge states, we again investigate the spatial distribution of the corresponding wave functions at the Γ point. The positions of the defect-induced states and the occupations are shown schematically in Fig. 10(d). The two-vacancy configuration induces four singlet states, all located below the ES region near the CBM. Three of the states are unoccupied and located at 0.1, 0.25, and 0.65 eV below the ES region, while the other singlet state is 1.0 eV below and is fully occupied. The three-vacancy configuration induces five singlet defect states below the ES region near the CBM. The lowest of these states is fully occupied and is located 1.0 eV below the ES region. The next highest state is 0.65 eV below the ES region and is occupied by one electron. The remaining three states are all unoccupied and are located 0.4, 0.35, and 0.1 eV below the ES region.

Comparing the two-vacancy result to that of the single vacancy, it can be seen that the two-vacancy configuration has one extra singlet state, with an extra electron populating the defect states. This results in a fully occupied state further below the ES region near the CBM, and the other three singlet states are unoccupied. The three-vacancy configuration has one extra singlet state than the two-vacancy configuration, with one electron populating this extra state. In Fig. 11(a) we plot the spatial distribution of the fully occupied defect state at the Γ point for the most favorable nitrogen two-vacancy configuration. This shows that it is mainly localized in the region of the vacancies, but there is also some "bulk-like" behavior with some of the spatial distribution on a number of the atoms, particularly nitrogen atoms both inside the wire and at the edges. In Fig. 11(b) we plot the

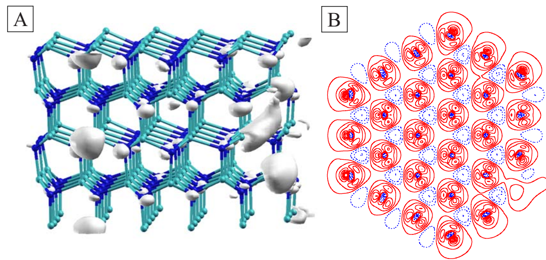

FIG. 11. (Color online) (a) The spatial distribution of the occupied defect state [see Fig. 10(d)] at the Γ point for the nitrogen two-vacancy configuration in the 216-atom nanowire. Nitrogen and gallium atoms are indicated by dark (blue) and light (aqua) spheres, respectively, and the orbitals are pale gray. (b) The difference electron-density distribution in the plane of one of the vacancies for the nitrogen two-vacancy configuration in the 216-atom nanowire. Solid (red) lines indicate charge accumulation and dashed (blue) lines indicate charge depletion.

difference electron-density distribution in the plane of one of the two nitrogen vacancies, which clearly shows an accumulation of charge at the site of the vacancies (a similar result is obtained when the difference electron-density distribution is examined in the plane of the second nitrogen vacancy).

The nitrogen vacancy is expected to be the major native point defect (as indicated by the lower formation energies for nitrogen vacancies compared to gallium vacancies) and so would contribute to the *n*-type conductivity of the nanowires. For the calculations with one and three nitrogen vacancies, we find an unpaired electron in a singlet state located at 0.5 and 0.65 eV below the ES region near the CBM, respectively. This appears consistent with recent electrical transport measurements of GaN nanowires[39] that suggest that the Fermi level is pinned at the surface of the nanowires at about 0.5–0.6 eV below the CBM.

2. Multiple Ga vacancies

To determine the energetically most favorable gallium two-vacancy configuration, we examine 20 different configurations in the 216-atom nanowire. The most stable configuration is shown in Fig. 12. The total formation energies for the two-vacancy configurations range from +6.8 to +14.4 eV (+3.4– +7.7 eV per vacancy), under gallium-rich conditions. As reported in Sec. II, under nitrogen-rich conditions, the total formation energies for the gallium two-vacancy configurations are smaller by −1.84 eV $(2\times\Delta H_f)$. Spin-polarized calculations of the most favorable vacancy configuration shows only a very small magnetic effect and results in a lowering of the total formation energy by 0.01 eV.

We first consider the formation energy per vacancy, for single and multiple vacancies at the center of the 216-atom nanowire (vacancies out-of-plane to each other in different gallium (0001) planes, but on nearest-neighbor sites), to see how this compares with the gallium vacancy in the bulk (in bulk GaN, the formation energy of the single Ga vacancy is 7.1 eV). The formation energy per vacancy for gallium vacancies at the center of the 216-atom nanowire is also 7.1 eV for both the one- and two-vacancy gallium configurations.

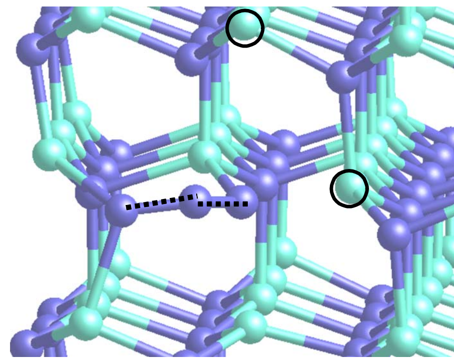

FIG. 12. (Color online) The most stable gallium two-vacancy configuration in the 216-atom nanowire. Nitrogen and gallium atoms are indicated by the dark (blue) and light (aqua) spheres, respectively. The open circles denote the location of the missing gallium atoms. The two dashed lines indicate nitrogen-nitrogen separation distances that are 1.30 and 1.41 Å.

This suggests that there is no significant interaction between the gallium vacancies at the center of the nanowire (in contrast to the nitrogen vacancy), although this does not mean there is not a favorable interaction between gallium vacancies located at the edge of nanowires. We investigate this in more detail below.

The most stable gallium two-vacancy configuration has both vacancies located close to each other at the edge of the nanowire but out-of-plane to each other in different gallium (0001) planes. This configuration of vacancies is the same as the most stable nitrogen two-vacancy configuration. Examining the total formation energies, the most stable two-vacancy configuration is 1.2 eV more favorable than the next most favorable configuration, which has the vacancies at the edge of the nanowire but in-plane [same gallium (0001) plane] with each other, and as close as possible to each other. When the two gallium vacancies are well separated but still at the edge of the nanowire, the configuration is 4.8 eV less stable than the most favorable configuration and when the two vacancies are at the center of the nanowire, the configuration in 6.5 eV less stable than the most favored one. This suggests, as found for the nitrogen two- and three-vacancy configurations, that there is an attractive interaction between vacancies as vacancies prefer to be clustered together rather than well separated, and they prefer to be at the edge of nanowires rather than in the bulk.

Examining the atomic geometry of the most stable two-vacancy configuration, we find that three nitrogen atoms neighboring the vacancies relax significantly to form an N_3 trimer-like configuration similar to an azide molecule. The N-N separations of the trimer-like species are 1.30 and 1.41 Å, significantly shorter than the N-N separation in bulk GaN of 3.28 Å but not as short as the calculated N-N bond length of 1.12 Å for the N_2 molecule or the average N-N bond length of 1.16 Å reported for the azide ion.[40] The Ga-N bond lengths for atoms at the edge of the wire that are involved in the N_3 trimer are notably elongated by 8.1–10.8 %, with respect to the bond lengths in the relaxed wire with no vacancies, indicating a reduced interaction of the nitrogen atoms with their gallium neighbors. Examining

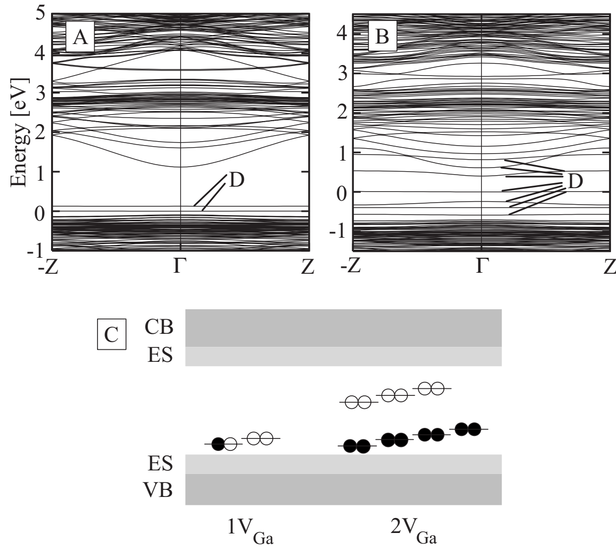

FIG. 13. Band structures of the most stable gallium (a) single vacancy and (b) two-vacancy configurations, with the energy zero set at the highest occupied state and defect states are labeled with a "D." (c) Corresponding schematic representation of the defect-induced levels for one and two gallium vacancies, where filled and open circles denote electrons and holes, respectively. "CB," "VB," and "ES" represent the conduction band, valence band, and edge states, respectively.

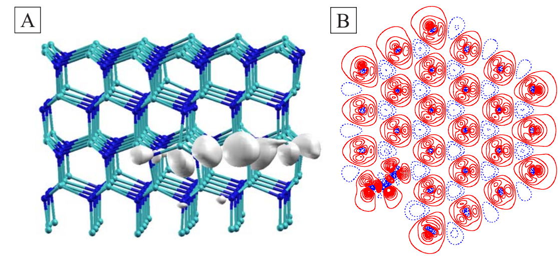

FIG. 14. (Color online) (a) The spatial distribution of the highest-energy fully occupied defect state [see Fig. 13(c)] at the Γ point for the gallium two-vacancy configuration in the 216-atom nanowire. Nitrogen and gallium atoms are indicated by dark (blue) and light (aqua) spheres, respectively, and the orbitals are pale gray. (b) The difference electron-density distribution in the plane of one of the vacancies for the gallium two-vacancy configuration in the 216-atom nanowire. Solid (red) lines indicate charge accumulation and dashed (blue) lines indicate charge depletion.

the Ga-N bond lengths for nitrogen atoms within an ∼4 Å radius of the trimer, we find a contraction of 1.8–2.5 %, with respect to the bond lengths in the relaxed wire with no vacancies. Nitrogen atoms ∼4–8 Å from the trimer experience a similar contraction in the Ga-N bond lengths of 4.8–9.6 %. This contraction may be explained by the reduced coordination of edge atoms, as a result of the formation of the trimer-like species.

The band structure of the most stable two-vacancy configuration is shown in Fig. 13(b) [that of the most stable single vacancy configuration is also shown in Fig. 13(a), for comparison]. To determine which states belong to the defect, the bulk or the edge states, we again investigate the spacial distributions of the wave functions at the Γ point. The positions of the defect-induced states and the occupations are shown schematically in Fig. 13(c).

The two-vacancy configuration induces seven defect singlet states spread out across the region of the band gap between the ES states near the VBM and CBM. The four lower singlet states are fully occupied and are located 0.1, 0.3, 0.45, and 0.7 eV, respectively, above the ES region near the VBM. The remaining three states are unoccupied and are located 1.1, 1.3, and 1.5 eV, respectively, above the ES region near the VBM. This behavior is quite different to that observed for the single gallium vacancy, where we find two defect-induced states just above the ES region near the VBM, with the lower of these two states occupied by one electron, while the higher of the two remains unoccupied. The significant reconstruction to form the N_3 trimer-like structure is the major difference between the most stable configurations. As a result of the reconstruction, there are extra dangling bonds around the vacancies that contribute to the extra defect-induced states we observe. In Fig. 14(a) we plot the spatial distribution of the highest-energy fully occupied defect state at the Γ point for the most favorable gallium two-vacancy configuration, where it can be seen that it is localized in the region of the vacancies. In Fig. 14(b) we plot the difference electron-density distribution in the plane of one of the two gallium vacancies, where an increase in electron density around the vacancies can be seen, and in particular, the increase in electron density on the N_3 trimer-like structure that forms in the vicinity of the vacancies is noticeable.

We can also examine the formation energy per vacancy to investigate whether as the number of vacancies increases, the configuration becomes more stable. The formation energy per vacancy for the most stable nitrogen one-, two-, and three-vacancy configurations ($1V_N^{wire}$, $2V_N^{wire}$, and $3V_N^{wire}$, respectively) in the nanowires and a single nitrogen vacancy in bulk GaN ($1V_N^{bulk}$) is 0.6, −0.2, −0.07, and 2.5 eV, respectively. So in order of stability, from the most favored to the least favored, we have $2V_N^{wire}$>, $3V_N^{wire}$>, $1V_N^{wire}$>, and $1V_N^{bulk}$. So per vacancy, it is easier to form the nitrogen two vacancy configuration than the three-vacancy configuration. Similarly, considering gallium vacancies, the formation energy per vacancy for the most stable gallium one- and two-vacancy configurations ($1V_{Ga}^{wire}$ and $2V_{Ga}^{wire}$, respectively) in the nanowires and a single gallium vacancy in bulk GaN ($1V_{Ga}^{bulk}$) is 5.9, 3.4, and 7.1 eV, respectively. So in order of stability, from the most favored to the least favored, we obtain $2V_{Ga}^{wire}$>, $1V_{Ga}^{wire}$>, and $1V_{Ga}^{bulk}$. Unfortunately the gallium three-vacancy configurations were not considered in this study, but the two-vacancy configuration in the nanowire is the most preferred for the gallium vacancies, as observed for nitrogen vacancies.

The implications from the formation energies for the single and multiple nitrogen and gallium vacancy configurations are that vacancies prefer to cluster than be well separated and that vacancies prefer to be located at the edges of the nanowires rather than in the center. We have also shown that nitrogen vacancies, at least in the neutral charge state, are more stable than gallium vacancies.

D. Single N and Ga vacancies: Effect of saturating wire edge dangling bonds with hydrogen

In Sec. III B, we considered single nitrogen and gallium vacancies in unsaturated nanowires. We now investigate the affect of saturating the wire edge dangling bonds with hydrogen. This is of interest as GaN nanowires that are produced under real growth conditions may be saturated by various molecules or species present in the growth environment. For these calculations, we use the 96-atom nanowire and consider the gallium and nitrogen vacancy in the center of the nanowire [site number 1 in Fig. 3(a)].

For the gallium vacancy, we find that the nitrogen atoms are displaced outward from the vacancy, with the Ga-N bond lengths of these atoms contracting by 2.9–7.6 % and 2.7–6.3 %, for the unsaturated and saturated nanowires, respectively (with respect to the Ga-N bond lengths in the relaxed unsaturated and saturated wires, with no vacancies). This suggests that saturating the edge dangling bonds with hydrogen has only a very small effect on the atomic relaxations. For a gallium vacancy in bulk GaN, we found a 2.9–3.7 % contraction (Sec. III A) in the Ga-N bond lengths of neighboring atoms; thus illustrating that the direction and magnitude of the atomic relaxations in the saturated and unsaturated wires are similar to those in the bulk.

For the nitrogen vacancy, the neighboring gallium atoms are displaced outward from the vacancy, with the Ga-N bond lengths of these atoms contracting by 0.2–1.7 % and 0.2–1.0 % for the unsaturated and saturated nanowires, respectively. This suggests, as found for the gallium vacancy in the center of the wire, that saturating the edge dangling bonds with hydrogen has only a very small affect on the atomic relaxations. In bulk GaN, a similar contraction of 0.2–0.3 % (Sec. III A) was found, thus again illustrating that the direction and magnitude of the atomic relaxations in the saturated and unsaturated wires are similar to those in the bulk.

The band structures of the unsaturated and saturated wires with a single gallium vacancy are illustrated in Figs. 15(a) and 15(b), respectively, and those of the unsaturated and saturated wires with a single nitrogen vacancy are illustrated in Figs. 15(c) and 15(d), respectively. As mentioned previously, we calculate the spatial distribution of the corresponding wave functions at the Γ point to determine whether they belong to the defect, the bulk, or edge states. The positions and occupations of the defect-induced states are shown schematically in Fig. 15(e).

For the gallium vacancy at the center of the unsaturated nanowire [Fig. 15(a)], we find three singlet states located just above the ES region near the VBM (0.15, 0.2, and 0.25 eV above), with the lowest of the singlet states fully occupied, the second lowest singlet containing one electron, and the highest singlet state unoccupied. We recall that the most stable configuration for a gallium vacancy is at the edge of the nanowire, where there are only two defect singlet states [Fig. 7(c)]. At the edge of the nanowire the coordination is less than in the center of the nanowire or in the bulk, so it is not surprising that the defect states differ when the vacancy is at the edge of the nanowire. At the center of the nanowire, the atoms are fully coordinated, so we can compare to the results for bulk GaN. In bulk GaN [Fig. 1(c)], there are three singlet states just above the VBM, with the lowest of the singlet states fully occupied, the second lowest singlet containing one electron and the highest singlet state unoccupied, which is qualitatively similar to what we find for the unsaturated nanowire with the defect in the center. For the saturated nanowire [Fig. 15(b)], the band gap is wider than for the unsaturated case [Fig. 15(a)]. We have reported previously that saturating dangling bonds removes their influence in the region of the band gap, leading to larger band gaps for the saturated nanowires.[15] The band gap of the saturated nanowires is also significantly greater than that of the bulk system (the band gaps are 2.7–0.4 eV larger than the bulk GaN band gap, for nanowires with diameters ranging from 6.3 to 35.0 Å). For the saturated nanowire, there is again three defect-induced states above the VBM; but compared to the unsaturated case, the three states are very close in energy (within ~0.02 eV difference, almost appearing as a triplet), and the states are further above the VBM (~0.5 eV). In bulk GaN, the energy separation of the three states above the VBM is ~0.1 eV, with the singlet states located 0.2–0.3 eV above the VBM.

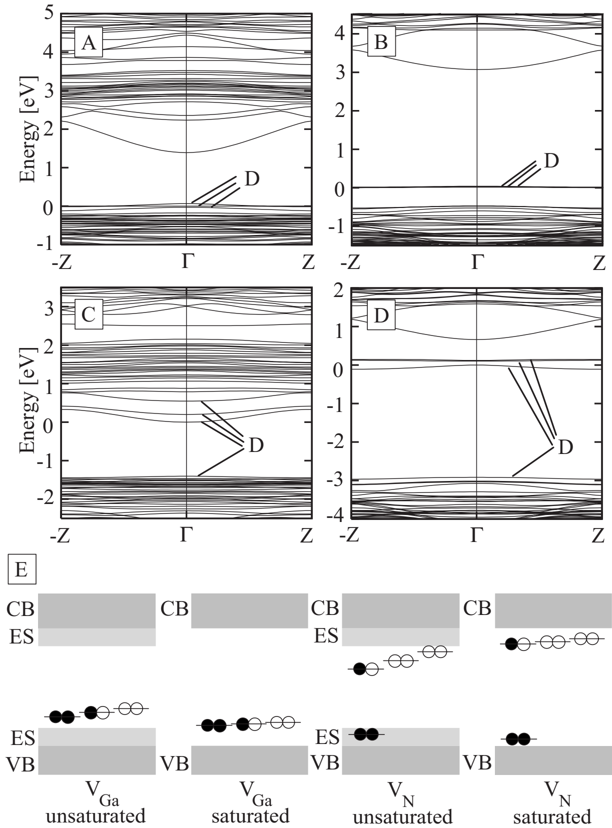

FIG. 15. The band structure for a gallium vacancy [site number 1 in Fig. 3(a)] in an (a) unsaturated and (b) saturated 96-atom nanowire. The band structure for a nitrogen vacancy [site number 1 in Fig. 3(a)] in an (c) unsaturated and (d) saturated 96-atom nanowire. The energy zero is set at the highest occupied state and defect states are labeled with a "D." (e) Corresponding schematic representation of the defect-induced levels for the vacancies in saturated and unsaturated nanowires, where filled and open circles denote electrons and holes, respectively. "CB," "VB," and "ES" represent the conduction band, valence band, and edge states, respectively.

For the nitrogen vacancy at the center of the unsaturated nanowire [Fig. 15(c)], there are four defect-induced singlet states, with one singlet state fully occupied, 0.1 eV below the ES region near the VBM, and three singlet states 0.25, 0.6, and 0.8 eV below the ES region near the CBM, with the lowest of these half occupied, and the other two unoccupied. As with the gallium vacancy, when we compare the results for the unsaturated nanowire with a vacancy in the center to the most stable configuration with the vacancy at the edge, we find that the vacancy at the edge has one less defect state [Fig. 5(c)]. In this case, the defect state just below the ES region near the VBM is not present when the vacancy is at the edge of the nanowire. The other (higher lying) defect states are similar, where both have three singlet defect states just below the ES region near the CBM. Comparing the defect-induced states of the unsaturated nanowire with the vacancy in the center to a nitrogen vacancy in bulk GaN [Fig. 1(c)] shows they are quite similar. Both induce four singlet defect states; but in bulk GaN, the unoccupied (highest) singlet state is just above the CBM, whereas in the unsaturated nanowire the unoccupied (highest) state is located just below the ES region near the CBM. For the saturated nanowire, there is again four defect-induced singlet states, with one singlet state fully occupied, 0.1 eV above the VBM, and three singlet states just below the CBM with the same occupations observed for the unsaturated wires, although in this case, the states are much closer together (0.5, 0.55, and 0.65 eV below the CBM). As with the unsaturated nanowire, when comparing the saturated nanowire to the results for bulk GaN, they compare closely, but with some small differences: the fully occupied defect state in the region of the VBM is actually located just above the VBM (in bulk GaN it is located just below the VBM) and the unoccupied (highest) singlet state is just below the CBM (while in bulk GaN it is located just above the CBM).

Overall there are some interesting differences between the results for the saturated and unsaturated wires with a single gallium and nitrogen vacancy in the center of the nanowire. While the atomic relaxations of neighboring atoms around each of the vacancies are similar (both in terms of magnitude and direction), the band structures are very different, as the unsaturated wires show edge states in the region of the VBM and CBM, while for saturated wires, the influence of the edge states has been removed. For the gallium vacancy, both the unsaturated and saturated nanowires contain three defect-induced singlet states, although in the unsaturated wire, the states are 0.15–0.25 eV above the ES region near the VBM, while in the saturated wire, the states are ~ 0.5 eV above the VBM and are very close together (within 0.02 eV). For the defect states induced by the nitrogen vacancy, both the unsaturated and saturated nanowires have four defect-induced singlet states, with the lowest (fully occupied) singlet 0.1 eV above the VBM in the saturated nanowire and 0.1 eV below the top of the ES region near the VBM for the unsaturated nanowire. The other three singlet states are all located near the CBM, with a separation of 0.25–0.8 eV below the ES region near the CBM for the unsaturated nanowires and a separation of 0.5–0.65 eV below the CBM for the saturated nanowires. On the basis of defect positions and occupancies, we find that nitrogen vacancies mainly act as donors and gallium vacancies act as acceptors. Interestingly, the fully occupied singlet state is located below the VBM in bulk GaN, while in the saturated nanowire it is located just above the VBM. This suggests that potentially the nitrogen vacancy in the saturated nanowire can act as a triple donor, while in bulk GaN it is a single donor.

IV. CONCLUSIONS

We have examined single and multiple gallium and nitrogen vacancies in unsaturated [0001] GaN nanowires, for two different sizes, namely, a 96-atom (9.5 Å diameter) and a 216-atom (15.9 Å diameter) nanowire. We find that the most stable location for a single gallium and nitrogen vacancy is at the edge of the nanowires. The most stable nitrogen two- and three-vacancy configurations are those where the vacancies are located at the edge of the nanowires and that the vacancies prefer to cluster together rather than be well separated. We also found this behavior for the most stable gallium two-vacancy configuration. A single gallium vacancy induces two singlet defect states above the ES region near the VBM, with the lowest of these occupied by one electron, and the other unoccupied. In bulk GaN, for the single gallium vacancy, there are three singlet defect states in a similar location, where the extra singlet state is fully occupied. For the gallium two-vacancy configuration, the band structure shows seven defect singlet states above the ES region near the VBM, with the four lower states fully occupied and the three remaining states unoccupied. There is a large reconstruction of the nitrogen atoms around the two gallium vacancies to form an N_3 trimer-like species, which gives rise to the extra states observed in the band gap. For a single nitrogen vacancy, there are three defect-induced singlet states located below the ES region near the CBM, with the lowest of these states occupied by one electron, while the other two defect states remain unoccupied. In bulk GaN, we find an extra singlet state that is fully occupied and located below the VBM and the highest unoccupied state is above the CBM. As for the single gallium vacancy, we attribute the missing singlet state to the lower coordination of the vacancy at the edge of the nanowire. For the nitrogen two-vacancy configuration, there are four singlet states below the ES region near the CBM, with the lowest of these fully occupied and the others unoccupied. We also find, as a result of relaxation around the two nitrogen vacancies, that there is a reduced distance (of 19.2%) between two gallium atoms, resulting in a Ga-Ga distance similar to in bulk Ga. For the nitrogen three-vacancy configuration, the induced defect states are similar to the most stable two-vacancy configuration, except that there is an extra singlet state and one more electron occupying these defect states.

We investigated the influence of saturating dangling bonds on the atomic and electronic properties of single gallium and nitrogen vacancies at the center of the nanowire. The band structures for the saturated and unsaturated cases have some notable differences, as the unsaturated wires show edge states in the region of the VBM and CBM, while for saturated wires, the influence of the edge states is removed. For the gallium vacancy, the unsaturated and saturated nano-

wires have three defect-induced singlet states, with the singlet states very close together in the saturated wires, almost appearing as a triplet state, while remaining slightly more spread out in the unsaturated wire. For the nitrogen vacancy in both the unsaturated and saturated nanowires, there are four defect-induced singlet states, with the lowest fully occupied singlet state located in the edge state region near the valence band in the unsaturated wire, and located above the VBM in the saturated wire.

Comparing the formation energies per vacancy of gallium defects versus nitrogen defects in the nanowires, we find that the nitrogen vacancy is considerably more stable (easier to form). Thus, we expect nitrogen vacancies to be the major native point defect in GaN nanowires, similarly to in bulk GaN.[10]

The nitrogen vacancy (and vacancy clustering) introduces occupied states ∼0.5–0.65 eV below the ES region near the CBM which may explain the experimentally reported pinning of the Fermi level at the nanowire surface, around 0.5–0.6 eV below the CBM. Furthermore, for unsaturated wires, the calculations indicate that any conductivity due to nitrogen or gallium vacancies will be confined to the outer region of the wires due to the close proximity of the defect-induced states to the ES bands.

ACKNOWLEDGMENTS

We gratefully acknowledge the Australian Partnership for Advanced Computing National Facility and the Australian Centre for Advanced Computing and Communications for their supercomputing facilities. This work was supported by the Australian Research Council.

*stampfl@physics.usyd.edu.au

[1] J. V. Barth, G. Costantini, and K. Kern, Nature (London) **437**, 671 (2005).
[2] C. M. Lieber and Z. L. Wang, MRS Bull. **32**, 99 (2007).
[3] J.-R. Kim, H. M. So, J. W. Park, J.-J. Kim, J. Kim, C. J. Lee, and S. C. Lyu, Appl. Phys. Lett. **80**, 3548 (2002).
[4] H.-J. Choi, H.-K. Seong, J. Chang, K.-I. Lee, Y.-J. Park, J.-J. Kim, S.-K. Lee, R. He, T. Kuykendall, and P. Yang, Adv. Mater. (Weinheim, Ger.) **17**, 1351 (2005).
[5] J. C. Johnson, H.-J. Choi, K. P. Knutsen, R. D. Schaller, P. Yang, and R. J. Saykally, Nature Mater. **1**, 106 (2002).
[6] C. G. Van de Walle and J. Neugebauer, J. Appl. Phys. **95**, 3851 (2004).
[7] J. Neugebauer and C. G. Van de Walle, Phys. Rev. B **50**, 8067 (1994).
[8] C. H. Park and D. J. Chadi, Phys. Rev. B **55**, 12995 (1997).
[9] S. Limpijumnong and C. G. Van de Walle, Phys. Rev. B **69**, 035207 (2004).
[10] M. G. Ganchenkova and R. M. Nieminen, Phys. Rev. Lett. **96**, 196402 (2006).
[11] Q. Wang, Q. Sun, and P. Jena, Phys. Rev. Lett. **95**, 167202 (2005).
[12] Q. Wang, Q. Sun, P. Jena, and Y. Kawazoe, Nano Lett. **5**, 1587 (2005).
[13] M.-H. Tsai, Z.-F. Jhang, J.-Y. Jiang, Y.-H. Tang, and L. W. Tu, Appl. Phys. Lett. **89**, 203101 (2006).
[14] A. Gulans and I. Tale, Phys. Status Solidi C **4**, 1197 (2007).
[15] D. J. Carter, J. D. Gale, B. Delley, and C. Stampfl, Phys. Rev. B **77**, 115349 (2008).
[16] M. Zhao, Y. Xia, X. Liu, Z. Tan, B. Huang, C. Song, and L. Mei, J. Phys. Chem. B **110**, 8764 (2006).
[17] P. Ordejon, E. Artacho, and J. M. Soler, Phys. Rev. B **53**, R10441 (1996).
[18] J. M. Soler, E. Artacho, J. D. Gale, A. Garcia, J. Junquera, P. Ordejon, and D. Sanchez-Portal, J. Phys.: Condens. Matter **14**, 2745 (2002).
[19] J. P. Perdew, K. Burke, and M. Ernzerhof, Phys. Rev. Lett. **77**, 3865 (1996).
[20] N. Troullier and J. L. Martins, Phys. Rev. B **43**, 1993 (1991).
[21] H. J. Monkhorst and J. D. Pack, Phys. Rev. B **13**, 5188 (1976).
[22] A. Gulans, R. A. Evarestov, I. Tale, and C. C. Yang, Phys. Status Solidi C **2**, 507 (2005).
[23] H. Schulz and K. H. Thiemann, Solid State Commun. **23**, 815 (1977).
[24] B. Monemar, Phys. Rev. B **10**, 676 (1974).
[25] J. Neugebauer and C. G. Van de Walle, Mater. Res. Soc. Symp. Proc. **339**, 687 (1994).
[26] J. Neugebauer and C. G. Van de Walle, Appl. Phys. Lett. **69**, 503 (1996).
[27] T. Mattila and R. M. Nieminen, Phys. Rev. B **55**, 9571 (1997).
[28] D. J. Carter and C. Stampfl (unpublished).
[29] B. Delley, J. Chem. Phys. **92**, 508 (1990).
[30] B. Delley, J. Chem. Phys. **113**, 7756 (2000).
[31] C. Stampfl and C. G. Van de Walle, Phys. Rev. B **59**, 5521 (1999).
[32] B. Delley, Phys. Rev. B **66**, 155125 (2002).
[33] J. E. Northrup and J. Neugebauer, Phys. Rev. B **53**, R10477 (1996).
[34] J. Neugebauer and C. G. Van de Walle, *Advances in Solid State Physics*, edited by R. Helbig (Vieweg, Braunschweig, 1996), Vol. 35, p. 25.
[35] T. Mattila and R. M. Nieminen, Phys. Rev. B **54**, 16676 (1996).
[36] Z. Wu, J. B. Neaton, and J. C. Grossman, Phys. Rev. Lett. **100**, 246804 (2008).
[37] X. M. Duan and C. Stampfl, Phys. Rev. B **77**, 115207 (2008).
[38] X. Y. Cui, X. Duan, D. Fernández-Hevia, and C. Stampfl (unpublished).
[39] R. Calarco, M. Marso, T. Richter, A. I. Aykanat, R. Meijers, A. V. D. Hart, T. Stoica, and H. Lüth, Nano Lett. **5**, 981 (2005).
[40] L. Tchertanov, Acta Crystallogr., Sect. B: Struct. Sci **55**, 807 (1999).